Global Change Biology (2005) **11,** 1–20, doi: 10.1111/j.1365-2486.2005.01059.x

Model-data synthesis of diurnal and seasonal CO_2 fluxes at Niwot Ridge, Colorado

WILLIAM J. SACKS*[1], DAVID S. SCHIMEL*, RUSSELL K. MONSON† and BOBBY H. BRASWELL‡

*Climate and Global Dynamics Division, National Center for Atmospheric Research, PO Box 3000, Boulder, CO 80307, USA,
†Department of Ecology and Evolutionary Biology, University of Colorado, Boulder, CO 80309, USA,
‡Complex Systems Research Center, University of New Hampshire, Durham, NH 03824, USA

Abstract

Eddy covariance records hold great promise for understanding the processes controlling the net ecosystem exchange of CO_2 (NEE). However, NEE is the small difference between two large fluxes: photosynthesis and ecosystem respiration. Consequently, separating NEE into its component fluxes, and determining the process-level controls over these fluxes, is a difficult problem. In this study, we used a model-data synthesis approach with the Simplified PnET (SIPNET) flux model to extract process-level information from 5 years of eddy covariance data at an evergreen forest in the Colorado Rocky Mountains. SIPNET runs at a twice-daily time step, and has two vegetation carbon pools, a single aggregated soil carbon pool, and a soil moisture submodel that models both evaporation and transpiration. By optimizing the model parameters before evaluating model-data mismatches, we were able to probe the model structure independent of any arbitrary parameter set. In doing so, we were able to learn about the primary controls over NEE in this ecosystem, and in particular the respiration component of NEE. We also used this parameter optimization, coupled with a formal model selection criterion, to investigate the effects of making hypothesis-driven changes to the model structure. These experiments lent support to the hypotheses that (1) photosynthesis, and possibly foliar respiration, are down-regulated when the soil is frozen and (2) the metabolic processes of soil microbes vary in the summer and winter, possibly because of the existence of distinct microbial communities at these two times. Finally, we found that including water vapor fluxes, in addition to carbon fluxes, in the parameter optimization did not yield significantly more information about the partitioning of NEE into gross photosynthesis and ecosystem respiration.

Keywords: eddy covariance, flux modeling, Markov chain Monte Carlo (MCMC) methods, model selection, net ecosystem exchange (NEE), parameter optimization, respiration, terrestrial carbon cycle

Received 2 July 2004; revised version received 17 November 2004; accepted 21 November 2004

Introduction

Understanding the environmental and substrate-level controls over respiration is central to predicting how terrestrial ecosystem carbon storage may change in the future. Unfortunately, it is rare that respiratory processes are measured explicitly at the ecosystem level (see Högberg *et al*., 2001; Subke *et al*., 2004 for examples of recent successes). Laboratory studies of soils and plants can provide insights into specific respiratory controls, but efforts to scale this insight up to ecosystems contain large uncertainties. Insight concerning respiratory processes is contained in the large set of eddy covariance data that are emerging from the numerous flux sites that constitute the Fluxnet global network (Baldocchi *et al*., 2001). One current challenge is to develop strategies to extract this insight using various modeling approaches that aim to partition the net CO_2 fluxes obtained from eddy covariance data, and even further, partition the component fluxes into under-

Correspondence: William J. Sacks, tel. +1 608 890 0337, fax +1 608 265 4113, e-mail: wsacks@wisc.edu
[1]Present address: Center for Sustainability and the Global Environment (SAGE), University of Wisconsin, 1710 University Avenue, Madison, WI 53726, USA

lying processes (e.g. Baldocchi & Wilson, 2001). For a number of reasons, this challenge is formidable. Ecosystem respiration is the sum of several components, classified into autotrophic and heterotrophic respiration. Within these two categories, different processes operate, including growth and maintenance respiration, and multiple substrate types can be used (Hanson *et al*., 2000). The first-order dependence of respiration on changing substrate availability can be difficult to separate from environmental regulation (Ryan & Law, 2005). This separation is further confounded when specific substrates are challenging to measure, especially true of organic matter fractions used by soil organisms for heterotrophic respiration.

Model-data synthesis techniques provide a new approach for gaining insights into the photosynthetic and respiratory components of net ecosystem CO_2 exchange and their regulation by climate and substrate availability (Schulz *et al*., 2001; Wang *et al*., 2001; van Wijk & Bouten, 2002; Braswell *et al*., 2005). As defined by Raupach *et al*. (2005), 'model-data synthesis' encompasses both parameter estimation and data assimilation. These techniques combine process-based models, observations of fluxes, and prior estimates of state and rate constants to assess which combinations of model structure and parameter values are most consistent with time-series observations. Rather than iteratively fitting each parameter to the subset of the data that best constrains that parameter – for example, first fitting respiration-related parameters to night-time CO_2 fluxes, then fitting photosynthesis-related parameters to the residual daytime fluxes – these techniques can consider all the data and all the parameters simultaneously. This allows greater consistency with the observations.

A number of recent studies have concluded that eddy covariance data contain information on the values of only three or four model parameters (Schulz *et al*., 2001; Wang *et al*., 2001). However, it is likely that this conclusion was only reached because of the short data record (2 or 3 weeks) used in these studies, a problem that Schulz *et al*. (2001) themselves acknowledged. Braswell *et al*. (2005) found that by using multiple years of eddy covariance data, a carbon flux model could be well constrained on most time scales of interest. Although there were 23 free parameters in this study, the majority of these parameters were well constrained by the CO_2 flux data.

In this study, we apply an ecosystem model and a Markov chain Monte Carlo (MCMC) parameter estimation approach to analyze a 5-year eddy covariance time series from the Niwot Ridge Ameriflux site (see Monson *et al*., 2002; Turnipseed *et al*., 2002 for a description of the site and its turbulent fluxes). We illustrate several ways in which model-data synthesis can be used to better understand the controls over the net ecosystem exchange of CO_2 (NEE), and in particular the respiration component of NEE. In our analyses, we focused primarily on areas of significant model-data mismatch, and on what we could learn about respiration in this ecosystem from these model failures. Although many modeling studies focus on agreements between the model and observations, model failures tend to be more informative than model successes. By performing a parameter optimization before assessing areas of model failure, we were able to probe the model structure independent of any given – and necessarily somewhat arbitrary – choice of parameters.

Most fundamentally, we ask the question, 'What is the best way of estimating the separate contributions of ecosystem respiration and photosynthesis to NEE?' As NEE is a fairly small difference between the large ecosystem respiration and photosynthesis fluxes, estimating the growing season daytime contribution of respiration to NEE is an important prerequisite for further analysis. Second, we use the technique to ask questions about seasonal mechanistic control over respiration by a combination of model selection (comparing the fit after small changes in model structure) and parameter value estimation. Through these analyses, we illustrate the types of information about respiration that are accessible through eddy covariance (CO_2 and H_2O) data, and also illustrate the synergisms between approaches involving empirical data collection and 'top-down' modeling. Specifically, we use a formal model selection criterion to attempt to answer the following questions: (1) are photosynthesis and foliar respiration down-regulated when soils are frozen? (2) Do the parameters governing soil respiration vary between summer and winter, supporting findings that suggest the existence of seasonally varying microbial communities at this site (Lipson *et al*., 2002)? (3) Is there more support for a soil respiration function that exhibits increasing temperature sensitivity with decreasing soil temperature (Lloyd & Taylor, 1994) than for a standard Q_{10} function? (4) Does the addition of a fast-turnover litter pool allow for more realistic model dynamics? (5) How much of an effect does soil moisture have on soil respiration at this site? Finally, we investigated the benefits of including H_2O fluxes as well as CO_2 fluxes in the optimization.

We used a relatively simple model in this study, partly to decrease the number of free parameters in the optimization and partly to allow for an easier diagnosis of the causes of model-data mismatch. We do not expect a simple model to capture all the observed scales of variability as it cannot include all the processes that affect CO_2 flux. If, on the other hand, we began with a sufficiently complex model of reasonably

appropriate structure, we could obtain a nearly perfect fit but it would be highly susceptible to over fitting (Gershenfeld, 1999). We, therefore, begin with a basic structure and only add complexity in response to specific hypotheses. After changing the model, we use a formal model selection statistic to evaluate the change in fit, to take into account changes in the dimensionality of the model. As will be discussed below, the model changes that we evaluate emerge from independent data and analyses at the site. That is, by beginning simple, we can identify systematic errors and use them as a guide to model development, rather than beginning with a complex model that, when used in an estimation framework, can likely be fit to the data so well that it will not generate informative errors.

Materials and methods

Data overview

The data used in this study were from the Niwot Ridge Ameriflux site, a high-elevation (3050 m), subalpine forest, located approximately 50 miles west of Boulder, Colorado (40°1′58″N; 105°32′47″W), just below the Continental Divide. The dominant species in this forest are subalpine fir (*Abies lasiocarpa*), Engelmann spruce (*Picea engelmannii*), and lodgepole pine (*Pinus contorta*). The forest is about 100 years old and is still in a state of aggradation, recovering from logging. The understory is relatively sparse, with 25% average coverage of tree seedlings, *Vaccinium* sp., lichens, and moss. Soils are sandy, with a thin (<6 cm) organic horizon. The annual precipitation averages 800 mm, and the mean annual temperature is 4 °C (Monson *et al*., 2002). The annual net primary productivity (NPP) of this site (250–500 g C m^{-2}) is lower than that of most forest ecosystems, owing to the harsh, high-elevation climate. This harsh climate restricts soil mineralization, plant growth, and the recruitment of new trees (Monson *et al*., 2002).

From November 1998 through the present, half-hourly fluxes of CO_2 and H_2O, along with corresponding climate data, have been measured at this site. For this study, we used data from November 1, 1998 through December 31, 2003. Fluxes were calculated using the eddy covariance method (Baldocchi *et al*., 1988; Baldocchi, 2003). Specific methods used at this site are described in a number of previous papers (Monson *et al*., 2002; Turnipseed *et al*., 2002, 2003, 2004). Briefly, CO_2 (or H_2O) flux estimates are calculated from the covariance of high-frequency fluctuations in vertical wind velocity and CO_2 (or H_2O) concentration. The NEE is defined as the sum of this flux term and a canopy CO_2 storage term, which is calculated from the change in CO_2 concentration as a function of height (Monson *et al*., 2002). Gaps in the flux data could occur either because of instrument malfunction or because of periods of high atmospheric stability ($u^* < 0.2$, which can lead to an underestimate of the flux; Goulden *et al*., 1996; Monson *et al*., 2002). Depending on the length of the gaps, they were filled using either a spline fit, empirical regressions based on photosynthetically active radiation (PAR), air and soil temperature, or a 10-day average (Monson *et al*., 2002). The total percentage of 30 min periods that required gap filling over the 5-year data set was 28% for the CO_2 flux data and 26% for the H_2O flux data.

We used six climate variables to drive the model's flux dynamics: (1) average air temperature, (2) average soil temperature, (3) precipitation, (4) flux density of PAR, (5) relative humidity, and (6) wind speed. Gaps in these climate drivers were filled using multivariate nonlinear regression (MacKay, 1992; Bishop, 1995) based on the available meteorological data, the day of year, and the time of day. The relative humidity and air temperature were then used to compute the atmospheric vapor pressure and the atmospheric vapor pressure deficit (VPD).

As the ecosystem model was run on a twice-daily time step, both the flux data and the climate drivers were aggregated up to two daily periods, where the exact length of each daytime or night-time step was based on the date. To avoid giving too much weight to gap-filled data points in the parameter optimization, only twice-daily time steps that were composed of at least 50% observed (i.e. not gap-filled) half-hourly fluxes were included in the optimization. This meant that 23% of the twice-daily CO_2 flux data points and 21% of the twice-daily H_2O flux data points were considered invalid. We did not require all half-hourly fluxes making up a time step to be observed, because doing so would allow only 30% of the twice-daily CO_2 flux data points to be included in the optimization, a significant loss of data. The optimization is somewhat sensitive to this threshold of the gap-filled fraction, although it remains unclear what is the best threshold to use (Braswell *et al*., 2005). We chose a 50% threshold as a compromise between a very strict and a very lenient threshold.

The Simplified PnET (SIPNET) ecosystem model

The ecosystem model that we used to model carbon and water fluxes was based largely on the PnET model developed by Aber and co-workers (Aber & Federer, 1992; Aber *et al*., 1995, 1996, 1997). We simplified a number of aspects of this model, for example replacing the carbon allocation scheme (Aber *et al*., 1996) with a simpler phenology model. To acknowledge the contri-

butions of PnET, we refer to our model as SIPNET. SIPNET describes carbon flux dynamics between the atmosphere and three terrestrial carbon pools: two vegetation pools – wood and leaves – and an aggregated soil carbon pool (Fig. 1). We do not explicitly separate aboveground and belowground autotrophic respiration, but include root respiration in the single autotrophic respiration term. Thus, we will use 'soil respiration' and 'heterotrophic respiration' interchangeably in this paper. Water flux dynamics are also modeled (Fig. 1), giving an estimate of evapotranspiration; soil wetness affects both photosynthesis and soil respiration. The model runs at a twice-daily time step, with one time step for each day or night. The initial conditions and fluxes governing the evolution of the model are controlled by 35 parameters, 32 of which were allowed to vary in the optimization (Table 1), and three of which were fixed (Table 2).

An earlier version of SIPNET, which was applied to a deciduous forest in the northeastern US (the Harvard Forest), is described by Braswell *et al*. (2005). We made two major changes to the model in applying it to the Niwot Ridge evergreen forest. First, we included a more complex water routine, incorporating evaporation and the modeling of a snow pack. This change was necessary because soil moisture is thought to be a significant determinant of NEE at Niwot Ridge (Monson *et al*., 2002); at Harvard Forest, in contrast, vegetation is thought to experience relatively less water stress (Aber *et al*., 1995). Snowmelt dynamics also have a significant effect on NEE at Niwot Ridge (Monson *et al*., 2002). Second, we used an evergreen leaf phenology rather than the deciduous phenology that was used in modeling the Harvard Forest. A summary of the major components of the model and a more complete description of the changes that have been made in this version are given in the appendix.

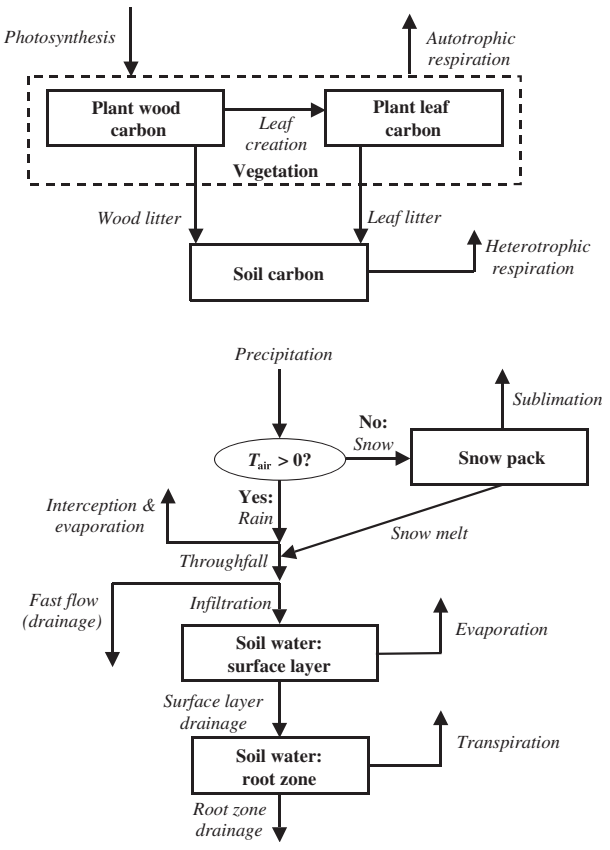

Fig. 1 Simplified PnET pools and fluxes. The model has two vegetation carbon pools and one soil carbon pool. The soil moisture submodel, which has been significantly expanded in this version of the model, includes two layers of soil water and a snow pack. Soil moisture affects both photosynthesis and soil respiration.

A driving philosophy in the design of this model was to include relatively few processes. In particular, we excluded processes for which the governing equations themselves are highly uncertain. Including such processes – and the accompanying additional parameters – could lead to an over fitting of the data that is not grounded in mechanistic understanding. Thus, for example, we did not explicitly model fine root dynamics because these dynamics are not well understood. Using a relatively simple model also made it easier to gain insights from model-data errors, and reduced the number of free parameters, thus decreasing the computational intensity of the optimization.

Parameter optimization

The parameter optimization method that we used is a variation of the Metropolis algorithm (Metropolis *et al*., 1953). The particular form of the algorithm that we used was described by Braswell *et al*. (2005); this algorithm was based on an algorithm developed by Hurtt & Armstrong (1996). The optimization algorithm generates not only a single best parameter set but also a range of parameter sets that represent approximately equally good matches to the data. This allows the generation of confidence intervals on the optimal parameter values, and the determination of correlations between parameters. In addition, by running the model forward on the retrieved ensemble of parameter sets, confidence intervals can be generated on the optimized model output.

In performing the optimization, each parameter was restricted to a specified allowable range (using a uniform prior distribution). Parameter ranges were determined through a combination of literature values, knowledge of the system, and initial tests of the optimization (Table 1). In general, we erred on the side of

Table 1 SIPNET parameters and initial conditions that were allowed to vary in the optimization, and their allowable ranges

Symbol	Definition	Range
Initial pool values		
$C_{W,0}$	Initial plant wood C content ($g\,C\,m^{-2}$)	6600–14 000
$C_{L,0}$	Initial plant leaf C content ($g\,C\,m^{-2}$)	0–630
$C_{S,0}$	Initial soil C content ($g\,C\,m^{-2}$)	3300–19 000
$W_{S,0}$	Initial soil moisture content, surface layer (fraction of $W_{S,c}$)	0–1
$W_{R,0}$	Initial soil moisture content, root zone (fraction of $W_{R,c}$)	0–1
Photosynthesis/respiration parameters		
A_{max}	Maximum net CO_2 assimilation rate ($nmol\,CO_2\,g^{-1}$ (leaf biomass) s^{-1})	0–34
K_F	Foliar maintenance respiration as fraction of A_{max} (no units)	0.05–0.30
T_{min}	Minimum temperature for photosynthesis (°C)	−8–8
T_{opt}	Optimum temperature for photosynthesis (°C)	5–30
Q_{10V}	Vegetation respiration Q_{10} (no units)	1.4–2.6
T_s	Soil temperature at which photosynthesis and foliar respiration are shut down (°C)	−5–5
K_{VPD}	Slope of VPD–photosynthesis relationship (kPa^{-1})	0.01–25
$PAR_{1/2}$	Half saturation point of PAR–photosynthesis relationship ($mol\,m^{-2}\,day^{-1}$)	7–27
k	Canopy PAR extinction coefficient (no units)	0.38–0.62
NPP_L	Fraction of NPP allocated to leaf growth (no units)	0–0.44
K_L	Turnover rate of leaf C ($g\,C\,g^{-1}\,C\,yr^{-1}$)	0–0.2
K_A	Wood respiration rate at 0 °C ($g\,C\,g^{-1}\,C\,yr^{-1}$)	0.0006–0.06
K_H	Soil respiration rate at 0 °C and moisture-saturated soil ($g\,C\,g^{-1}\,C\,yr^{-1}$)	0.006–0.15
Q_{10S}	Soil respiration Q_{10} (no units)	1.4–3.5
Moisture parameters		
f	Fraction of soil water removable in one day (no units)	0.001–0.16
K_{WUE}	VPD–water use efficiency relationship ($mg\,CO_2\,kPa\,g^{-1}\,H_2O$)	0.01–30
$W_{S,c}$	Soil water-holding capacity, surface layer (cm (precipitation equivalent))	0.01–4
$W_{R,c}$	Soil water-holding capacity, root zone (cm (precipitation equivalent))	0.1–36
E	Fraction of rain immediately intercepted and evaporated (no units)	0–0.2
F	Fraction of water entering soil that goes directly to drainage (no units)	0–0.2
K_S	Snow melt rate (cm (water equivalent) $°C^{-1}\,day^{-1}$)	0.05–0.25
K_D	Rate of water drainage from upper to lower soil water layer for fully saturated upper layer (cm (water equivalent) day^{-1})	0.01–1.0
R_d	Scalar relating aerodynamic resistance to wind speed (no units)	60–1500
$R_{soil,1}$	Scalar relating soil resistance to fractional soil wetness (see text) (no units)	0–16.4
$R_{soil,2}$	Scalar relating soil resistance to fractional soil wetness (see text) (no units)	0–8.6
Tree physiological parameters		
SLW_C	C content of leaves on a per area basis ($g\,C\,m^{-2}$ (leaf area))	86–500
K_W	Turnover rate of plant wood C ($g\,C\,g^{-1}\,C\,yr^{-1}$)	0.003–0.3

The ranges assume a uniform prior distribution.

making the parameter ranges too wide, to try to ensure that the ranges included the actual value and to give the optimization more freedom. Initial guesses for the parameters were also derived from a combination of literature values and knowledge of the system, but we did not place much emphasis on choosing the 'correct' value of the parameters because it has been found that this method of parameter optimization is relatively insensitive to the parameters' initial values (Braswell *et al*., 2005).

The optimization proceeds as a quasi-random walk through the parameter space, attempting to find parameter sets that minimize the model-data error. Here, model-data error is defined in terms of likelihood (L), and minimizing this error is equivalent to maximizing the likelihood:

$$L = \prod_{i=1}^{n} \frac{1}{\sqrt{2\pi}\sigma} e^{-(x_i-\mu_i)^2/2\sigma^2}, \quad (1)$$

where n is the number of data points, x_i and μ_i are the measured and modeled fluxes, respectively, and σ is the error (one standard deviation) on each data point. It is important to note that here σ represents data error *relative to the given model structure*, and thus represents a combination of measurement error and process representation error. In practice, log likelihood (LL) is used in place of likelihood as it is computationally easier to work with. As mentioned above, we only used

Table 2 SIPNET parameters that were held constant in the optimization

Symbol	Definition	Value	Source
$W_{P,0}$	Initial snow pack (cm, water equivalent)	0	N/A
F_{Amax}	Average daily max photosynthesis as fraction of A_{max} (no units)	0.76	Aber *et al*. (1996)
F_C	Fractional C content of leaves ($g\,C\,g^{-1}$ (leaf biomass))	0.45	Aber *et al*. (1995)

The two parameters F_{Amax} and F_C could not be estimated independent of other model parameters.
N/A, not applicable.

twice-daily data points for which at least 50% of the half-hourly values making up the data point were measured (i.e. not gap-filled).

Note that this likelihood equation assumes a Gaussian model-data error, and a uniform σ for all data points. We acknowledge that these assumptions may be violated for eddy covariance data. For example, night-time fluxes may have larger errors, especially in complex terrain like that at our study site, due in part to cold air drainage, although the application of a u^* filter (see Data Overview) should correct for this problem (Goulden *et al*., 1996; Monson *et al*., 2002). In addition, even during ideal conditions, it is likely that there may have been some systematic errors (Goulden *et al*., 1996). Finally, it should be noted that in computing the likelihood, we used cumulative fluxes over each twice-daily time step rather than rates. This distinction is meaningful because the time steps could vary in length by a few hours. Whether this choice made the assumption of constant σ more or less valid is unclear, and depends on the error structure of the data. However, a detailed error analysis was beyond the scope of this study.

Because σ is unknown, we estimated σ at each step of the optimization. For a given model output (i.e. a given set of μ_i values), we determine the most likely value of σ, or the value that maximizes L (Hurtt & Armstrong, 1996), which is

$$\sigma_e = \sqrt{\frac{1}{n}\sum_{i=1}^{n}(x_i - \mu_i)^2}. \quad (2)$$

Braswell *et al*. (2005) found that the values of σ_e retrieved from optimizations on synthetic data sets, generated by running the model forward using known parameter values and then adding Gaussian error, matched the values used to generate the data sets almost exactly. This finding lends validity to our method of estimating σ.

For most experiments, we used only the CO_2 fluxes in the optimization. That is, the x_i terms were measured NEE fluxes, and the μ_i terms were modeled NEE fluxes. Modeled NEE is given by

$$NEE = R_A + R_H - GPP, \quad (3)$$

where R_A is the autotrophic respiration, R_H is the soil (i.e. heterotrophic) respiration, and GPP is the gross primary productivity. In one experiment, however, we used both CO_2 fluxes and H_2O fluxes in the optimization. The observed H_2O fluxes were compared with modeled evapotranspiration (ET):

$$ET = E_I + E_P + E_S + T, \quad (4)$$

where E_I is immediate evaporation, E_P is sublimation from the snow pack, E_S is soil evaporation, and T is transpiration (see appendix for a description of these fluxes). In performing the optimization in this experiment, the total likelihood (L_{tot}) was given by

$$L_{tot} = L_{CO_2} L_{H_2O}, \quad (5)$$

where L_{CO_2} is the likelihood derived from considering only the model-data error in net CO_2 flux, and L_{H_2O} is the likelihood derived from considering only the model-data error in H_2O flux. This formulation implies that the two partial likelihood terms are independent. In particular, note that each of these partial likelihood terms uses a different value for σ_e, the estimated data standard deviation (relative to the model) for a given data type, allowing for a dynamic weighting of the two data types.

Each step of the optimization consists of choosing a parameter (P_i) at random and changing its value by a random amount, keeping all other parameters fixed at their previous values. The model is run using the newly generated parameter set, and its likelihood, L(new), is compared with the likelihood of the previous point, L(old). If $L(\text{new}) \geq L(\text{old})$, the new parameter set is accepted. If $L(\text{new}) < L(\text{old})$, the new parameter set may still be accepted; the probability of acceptance is the ratio of the likelihoods. If the new parameter set is rejected, the new point is ignored and P_i reverts to its old value. The acceptance of parameter sets that yield slightly worse likelihoods helps prevent the optimization from getting stuck in local, but nonglobal, optima. After a spin-up period (described in Braswell *et al*., 2005), the set of accepted points is an estimator of the posterior distribution of the parameters. In this study,

we ran the optimization long enough to generate about 150 000 such accepted points.

Experiments involving model modification

Our overall experimental strategy was to make modifications to the structure of the model and test whether these modifications improved the model-data fit in the face of an optimized parameter set. We made five modifications to the model described in the appendix. By examining the effect of these modifications on the model-data fit, we expected to learn more about the controls on NEE in this ecosystem. We were especially interested in the dynamics of soil respiration, so four of the five modifications related to the soil respiration component of SIPNET. A parameter optimization such as the one used in this study allows for a more robust model selection. With a single, somewhat arbitrary set of parameters, mismatches between model predictions and validating data must be interpreted as being because of a combination of (1) data error, (2) error in model structure (i.e. representation of processes within the model), and (3) cumulative errors because of parameter values being displaced from optimality. Parameter optimization allows us to evaluate the ability of the model to represent the data after minimizing the third source of error; thus, we can better isolate the influence of model structure (Braswell *et al*., 2005).

In the first modification, we forced the net photosynthetic rate to zero when the soil temperature fell below a threshold temperature, T_S. Although the forest at Niwot Ridge is mostly evergreen, photosynthesis rates are close to zero during the winter, even when air temperatures are relatively high (Monson *et al*., 2002). Similar findings have been reported in other cold-climate evergreen forests (Hollinger *et al*., 1999). A suggested mechanism is the lack of available water for transpiration when the soil is frozen (Hollinger *et al*., 1999; Monson *et al*., 2002). In addition, because there is little or no fresh photosynthate supplied to leaves in the winter, it is likely that foliar respiration is reduced to near-zero as well. In support of this hypothesis, Hollinger *et al*. (1999) found that in a spruce-dominated forest, below-canopy CO_2 flux accounted for nearly all the nocturnal respiration in the winter. We tested this hypothesis by turning the photosynthetic and foliar respiration fluxes off entirely during the winter. The timing of this shutdown was based on a soil temperature threshold, T_S, which we allowed to vary in the optimization because of uncertainties regarding the mechanisms responsible for this shutdown.

Because this first modification led to significant improvements in the model-data fit (see Results), we used this version as the base on which the remaining four modifications were made. Thus, we will use 'base model' to refer to the model with this single modification. The remaining four modifications were made independent of each other – that is, each model version had only one modification in place.

In the second modification ('seasonal R_H model'), we replaced the single set of parameters governing soil respiration (K_H and Q_{10S}) with two such sets of parameters: one set governing soil respiration during the summer when the soil is warm ($K_{H,w}$ and $Q_{10S,w}$) and the other during the winter when the soil is cold ($K_{H,c}$ and $Q_{10S,c}$). The allowed ranges of these parameters were the same as for the similar parameters in the base model, except for $Q_{10S,c}$, which had a higher upper limit (6.0). The temperature below which the cold-soil parameters were used was determined by a third new parameter (T_c; range: -2 to 4 °C). Lipson *et al*. (2002) found evidence for the existence of seasonally varying microbial communities in an ecosystem near our study site, and preliminary measurements at our study site have revealed evidence for two distinct seasonal microbial communities as well (Lipson, Scott-Denton & Monson, unpublished data). The allowance for seasonally varying respiration parameters in the model was meant partly as a test of these findings and partly as an investigation of how much of the model-data error could be corrected by allowing such seasonal variations.

In the third modification ('Lloyd-and-Taylor model'), we replaced the Q_{10} function relating soil respiration to soil temperature with an alternative formulation that has been found to produce a better fit to soil respiration data (Lloyd & Taylor, 1994, their Eqn (11)):

$$f(T_{soil}) = e^{E_0\left(\frac{1}{-T_0}-\frac{1}{T_{soil}-T_0}\right)}, \quad (6)$$

where T_{soil} is the soil temperature, and E_0 and T_0 are empirical parameters. As E_0 and T_0 are highly correlated, we fixed E_0 at 309 (Lloyd & Taylor, 1994), and allowed T_0 to vary across a wide range of values (-273 to -25 °C; Lloyd & Taylor (1994) give -46 °C), as was done in Falge *et al*. (2001). Note that this model implies increasing temperature sensitivity with decreasing temperatures. This modification tested whether a more parsimonious model could achieve the same results as the seasonal R_H model.

In the fourth modification ('litter model'), we replaced the single aggregated soil carbon pool with two pools: an upper litter pool and a lower soil pool. Wood and leaf litter were added to the upper litter pool. Litter breakdown was computed using the same functional form as soil respiration (see appendix), but with a different base rate (K_B; range: 0.1–1.6 g C g^{-1} C yr^{-1}), and using the surface layer moisture content rather

than that of the root zone; the temperature effect remained the same. An additional parameter governed the fraction of broken-down litter that was respired (F_R; range: 0.25–0.75), with the remainder being transferred to the lower soil carbon pool. A third additional parameter specified the initial carbon content of the litter pool (range: 130–1200 g C m^{-2}). This modification was meant to test how much better the model could match the data with the additional substrate dynamics allowed by this litter pool.

In the fifth modification ('moisture-independent R_H model'), soil respiration was made independent of soil moisture. This modification was meant to test the importance of the moisture effect on soil respiration in this ecosystem.

Results

Optimization on base model

The monthly mean residuals generated using the best parameter set from the optimization, and using the model without the shutdown of either photosynthesis or foliar respiration in the winter, are shown in Fig. 2a. An examination of these residuals recommends the inclusion of these shutdown effects in the model. During the winter months, this model predicts too much respiration at night, and too much photosynthesis during the day (although this latter difference could also be due to predicting too little respiration during the day). During the growing season, the model predicts too little respiration at night and too little photosynthesis (or too much respiration) during the day. When photosynthesis and foliar respiration are shut down in the winter (in the 'base model'), the optimized model-data fit is significantly better than the optimized fit on the model without these shutdowns (Table 3). Although the monthly mean model-data residuals show similar patterns for both models, they are generally of a lesser magnitude for the model that includes the winter down-regulation (Fig. 2b). An optimization on a model that included the wintertime shutdown of photosynthesis but not foliar respiration showed most, but not all, of the improvement seen in the model with a shutdown of both (data not shown). It is also interesting to note that the optimized value of T_S tended to be within half a degree of 0 °C. These results lend support to the hypothesis that frozen soils cause a shutdown of at least photosynthesis, and possibly also foliar respiration (Hollinger *et al*., 1999; Monson *et al*., 2002).

The best parameter set retrieved from the optimization on the base model is shown in Table 4. The posterior distribution of each parameter is also given, indicating how well the observations constrain each parameter. The modeled NEE time series generated with the base model, using the best parameter set retrieved from the optimization, along with the observed time series, are shown in Fig. 3. The optimized model matches the general patterns in the data well, but overlooks some significant features. First, the model does not capture the peak summertime uptake evident in the data. The largest errors occur during the months of May and June (Fig. 2b), when the forest exhibits high photosynthetic rates because of a relative lack of water limitation. This error may represent a compromise that the optimization makes to match both the high uptake rates early in the growing season and the relatively lower uptake rates in mid-summer, when there is more water limitation.

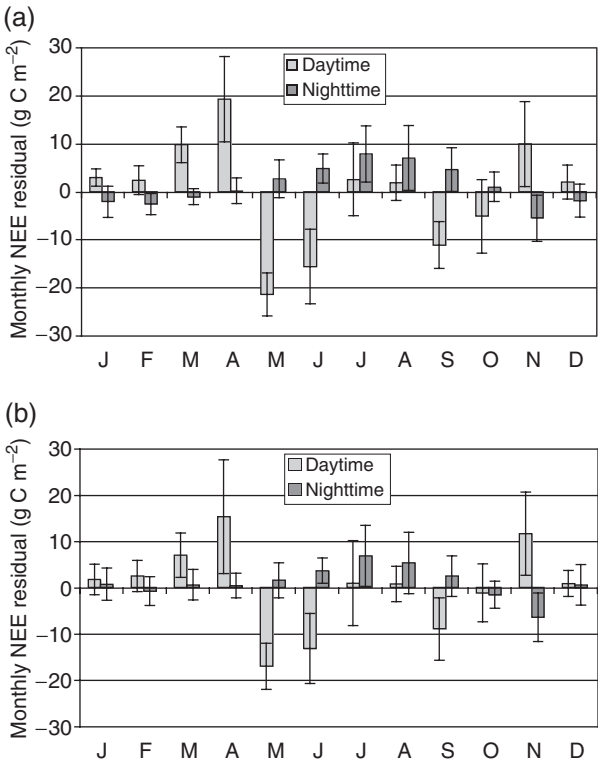

Fig. 2 Monthly mean residuals (data minus model) generated using the best parameter set retrieved from the optimization, using (a) a model without wintertime down-regulation of photosynthesis or foliar respiration, and (b) a model with these down-regulations ('base model'). Error bars show one standard deviation of the five (for January–October, 1999–2003) or six (for November and December, 1998–2003) annual means for each month. Positive net ecosystem exchange of CO_2 denotes net loss of CO_2 from the ecosystem to the atmosphere. Note that the residuals are generally in the same direction for both models, but tend to be smaller for the model with wintertime down-regulation of photosynthesis and foliar respiration.

Table 3 Model-data comparison statistics from running six versions of SIPNET using the best parameter set retrieved from the optimization on each model

	Base model	No winter time shutdown of psn., foliar resp.	Seasonal R_H	Lloyd-and-Taylor model	Add'l litter pool	Moisture-independent R_H
Best log likelihood*	−2404.2	−2614.7	−2374.0	−2403.2	−2407.6	−2415.7
RMS error†	0.555	0.597	0.550	0.555	0.556	0.558
# free parameters	32	31	35	32	35	32
BIC‡	5063.4	5476.5	5027.0	5061.5	5094.1	5086.4

See text for a description of model variations.
*Larger (i.e. closer to zero) numbers mean greater likelihood.
†Root mean square error in $g\,C\,m^{-2}$ over a single time step.
‡BIC (Bayesian Information Criterion) = $-2\,LL + K \ln(n)$, where LL is the log likelihood, K is the number of free parameters, and n is the number of data points used in optimization (2894). A lower BIC indicates a model with greater support from the data.

Second, the model is not able to capture the most significant periods of mid-summer NEE reduction. This is most noticeable in 2002, when the data show a period of net carbon loss to the atmosphere in the middle of the growing season (Fig. 3b). This period of net loss is presumably because of a combination of high temperatures allowing higher respiratory rates (as is evident from the high night-time NEE, Fig. 3a), and low soil moisture levels causing a decrease in photosynthesis. The winter of 2002 was the driest on record for this region over more than 100 years of climate records. The extremely low amount of wintertime precipitation, and lower-than-normal summertime precipitation, left the midsummer soils in an extremely dry state. The optimized model, however, predicts no water stress at this time (Fig. 4).

Third, the model is not able to match the observed variability in night-time respiration (Fig. 5). This error is particularly apparent in the model's inability to match the highest levels of respiration observed in the data (Figs 2b and 3d).

The model reproduces the basic features of the seasonal and diurnal cycle of NEE (Fig. 6). In general, the differences between the modeled and observed diurnal cycles lie within the range of annual variability. This is consistent with SIPNET results at the Harvard Forest, where the model also accurately simulated the seasonal and diurnal cycle amplitudes (Braswell *et al*., 2005). The model is consistently biased, however, slightly underestimating diurnal amplitude in the summer but slightly overestimating diurnal amplitude in the spring and fall. Some of the error in simulating the diurnal cycle likely emerges from the model's failure to capture peak daytime uptake rates and the full range of observed night-time respiration rates.

One of the advantages of the optimization method used in this study is that it generates an ensemble of parameter sets that represent approximately equally good matches between model and data. By running the model forward using each parameter set in this ensemble, it is straightforward to generate uncertainty estimates on the model's predictions (Fig. 7). In this case, the model uncertainty is small relative to the model-data error. Thus, as in the above analysis, we can take the model predictions generated using the single best parameter set to be fairly representative of the patterns seen using any parameter set in the ensemble. Consequently, in further analyses we will consider only the best parameter set retrieved from the optimization, unless otherwise noted.

Optimization on multiple data types

In performing a simultaneous optimization on 32 parameters, it is likely that there will be tradeoffs between some parameter pairs. That is, by varying two parameters together, the optimization could achieve an equally good model-data fit, or possibly even an almost identical model output. In such cases, neither parameter value can be estimated accurately. As the optimization provides an ensemble of parameter sets that represent good fits of the model to the observations, it can be used to investigate such parameter correlations. We do, in fact, find high linear correlations between a number of parameter pairs (Fig. 8). For example, A_{max} (the maximum net CO_2 assimilation rate) and $PAR_{1/2}$ (the half saturation point of the PAR–photosynthesis relationship) were positively correlated ($r = 0.58$), suggesting that these two parameters could be increased (or decreased) simultaneously and the model's NEE predictions would not vary significantly. There were also a number of high correlations between rate constants and initial conditions. For example, K_H and $C_{S,0}$ were negatively correlated ($r = -0.89$). This points out the diffi-

Table 4 Parameter values retrieved from the optimization on the base model (see Table 1 for parameter definitions)

Parameter	Best value	Mean value
$C_{W,0}$ (g C m^{-2})	7432	8071 ± 1374
$C_{L,0}$ (g C m^{-2})	564	521 ± 91
$C_{S,0}$ (g C m^{-2})	18 889	14 666 ± 3809
$W_{S,0}$	0.03	0.07 ± 0.07
$W_{R,0}$	0.02	0.02 ± 0.01
A_{max} (nmol CO$_2$ g^{-1} s^{-1})	7.66	9.15 ± 1.85
K_F	0.28	0.217 ± 0.034
T_{min}(°C)	−1.95	−1.93 ± 0.17
T_{opt}(°C)	18.3	18.5 ± 0.9
Q_{10V}	2.44	2.29 ± 0.12
T_s(°C)	−0.32	−0.34 ± 0.01
K_{VPD} (kPa^{-1})	0.094	0.099 ± 0.006
$PAR_{1/2}$ (mol m^{-2} day^{-1})	7.9	10.2 ± 1.5
k	0.525	0.495 ± 0.068
NPP_L	0.021	0.016 ± 0.014
K_L (g C g^{-1} C yr^{-1})	0.037	0.037 ± 0.011
K_A (g C g^{-1} C yr^{-1})	0.023	0.028 ± 0.005
K_H (g C g^{-1} C yr^{-1})	0.009	0.010 ± 0.003
Q_{10S}	1.50	1.52 ± 0.10
f	0.028	0.026 ± 0.010
K_{WUE} (mg CO$_2$ kPa g^{-1} H$_2$O)	29.1	24.8 ± 3.6
$W_{S,c}$ (cm)	3.66	3.48 ± 0.47
$W_{R,c}$ (cm)	22.1	23.0 ± 4.2
E	0.090	0.095 ± 0.057
F	0.066	0.100 ± 0.056
K_S (cm °C^{-1} day^{-1})	0.068	0.079 ± 0.020
K_D (cm day^{-1})	0.01	0.07 ± 0.12
R_d	101	138 ± 51
$R_{soil,1}$	8.6	11.7 ± 3.0
$R_{soil,2}$	0.004	2.20 ± 2.05
SLW_C (g C m^{-2})	231	368 ± 95
K_W (g C g^{-1} C yr^{-1})	0.29	0.21 ± 0.05

The 'Best value' column reports the parameter set that yielded the highest likelihood in the Markov chain Monte Carlo parameter estimation. The 'Mean value' column reports the estimated posterior mean and standard deviation of each parameter, generated from 168 150 parameter sets that yielded approximately equally good model-data fits.

culty in separating direct climatic controls over NEE from indirect controls such as the influence of substrate availability on respiration rate (Giardina & Ryan, 2000; Ryan & Law, 2005).

Another type of correlation arises in this optimization because of the particular data we used. NEE is the relatively small difference between two large fluxes: ecosystem respiration (R) and GPP. Thus, it is easy for the model to achieve the right answer (i.e. a good match to the observed NEE) for the wrong reasons (i.e. wrong partitioning of NEE into component fluxes, for example by overestimating both R and GPP). The effects of both the parameter correlations and these correlations between component fluxes could – in principle – be reduced by optimizing on multiple data types. Increasing two parameters simultaneously may result in similar model predictions of the first data type without resulting in similar predictions of the second data type. Similarly, a second data type could allow a better separation of GPP and R. We tested the effect of including a second data type by optimizing on water vapor fluxes in addition to net CO_2 fluxes. During the day, H_2O fluxes are primarily influenced by transpiration, and thus by the level of gross photosynthesis, so these fluxes could provide a means for separating GPP and R.

Not surprisingly, optimizing on both data types led to a large decrease in the model-data error in H_2O flux (CO_2 alone: root mean square (RMS) error = 0.150 cm precipitation equivalent over a single time step; both data types: RMS error = 0.062 cm precipitation equivalent over a single time step), but a slight increase in the model-data error in net CO_2 flux (CO_2 alone: RMS error = 0.555 g C m^{-2} over a single time step; both data types: RMS error = 0.569 g C m^{-2} over a single time step). When optimizing on two data types, we can no longer achieve the best possible match of either data type individually. In addition, in the optimization on both data types there was a general decrease in the posterior variances of parameters that directly influence the H_2O flux. The variances of other parameters were neither consistently larger nor consistently smaller than in the optimization on CO_2 alone.

The inclusion of H_2O fluxes in the optimization did not significantly change the number of highly correlated parameters (Fig. 8). Most of the highly correlated parameters in the optimization on CO_2 alone were still highly correlated when H_2O fluxes were included in the optimization. Moreover, the inclusion of H_2O fluxes in the optimization did not lead to a significantly different optimal separation of NEE into GPP and R, although it did lead to a different separation of R into autotrophic respiration (R_A) and heterotrophic respiration (R_H) (Fig. 9). Wood respiration rates were significantly higher, and heterotrophic respiration rates significantly lower, in the optimization on both data types. The mean annual NPP in the optimization on CO_2 fluxes alone was 273 g C m^{-2} (with a range of 229–318 g C m^{-2} over the 5 years, 1999–2003), while the mean NPP in the optimization on both fluxes was 145 g C m^{-2} (with a range of 123–193 g C m^{-2} over the 5 years). Most of this difference was because of the different partitioning of R into R_A and R_H. Monson *et al*. (2002) estimate the annual NPP in this forest to be between 250 and 500 g C m^{-2}. The NPP estimated from the optimization on CO_2 fluxes alone generally falls within this range, while the NPP estimated from the

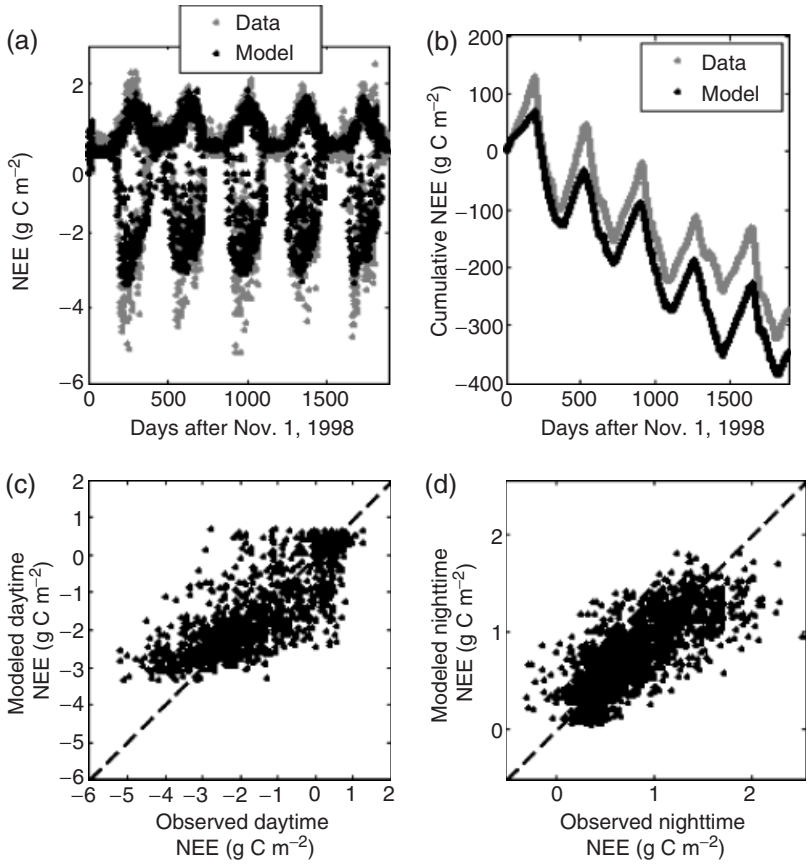

Fig. 3 Model-data comparisons using the base model run with the best parameter set retrieved from the optimization. (a) and (b) show the time series and cumulative time series, respectively, of twice-daily modeled and observed net ecosystem exchange of CO_2 (NEE), from November 1, 1998 to December 31, 2003. (c) and (d) show modeled vs. observed NEE for daytime and night-time points, respectively. Positive NEE denotes net loss of CO_2 from the ecosystem to the atmosphere. Major errors between the model and observations are (1) the model underestimates the peak summertime CO_2 uptake, (2) the model does not capture the mid-summer NEE reduction in 2002, and (3) the model underestimates the peak night-time respiration rates.

optimization on both fluxes does not. Thus, forcing the model to match H_2O fluxes actually caused the partitioning of respiration, and as a result NPP, to become less realistic.

Model modifications

The optimization on the seasonal R_H model yielded a better model-data fit than that on the base model (Table 3). With three additional parameters, however, this optimization is expected to perform somewhat better simply because of the additional degrees of freedom in the fit. The Bayesian Information Criterion (BIC) allows one to account for the effect of these additional parameters (Kendall & Ord, 1990):

$$\mathrm{BIC} = -2\mathrm{LL} + K\ln(n), \quad (7)$$

where LL is the log likelihood, K is the number of free parameters in the model, and n is the number of data points used in the optimization (in this case, 2894). The model with the lower BIC is considered to be better. Even after accounting for the greater number of parameters in this way, the seasonal R_H model is still judged to be slightly better than the base model (Table 3).

The improved performance of this modified model is achieved by introducing significant differences in both the base respiration rates ($K_{H,w}$ and $K_{H,c}$) and the respiration Q_{10S} ($Q_{10S,w}$ and $Q_{10S,c}$) in warm and cold soils (Table 5). The retrieved base respiration rate in warm soils was slightly lower than the base rate in the model with a single set of soil respiration parameters, and the retrieved rate in cold soils was significantly higher. Both retrieved Q_{10S} in the modified model were higher than the Q_{10} in the base model. The retrieved Q_{10} in cold soils was significantly higher than that in warm soils, consistent with process studies in cold region soils (Mikan *et al*., 2002). The mean monthly differences in predicted NEE between the seasonal R_H model and the base model show the same general patterns for both daytime and night-time points. At both times of day, the

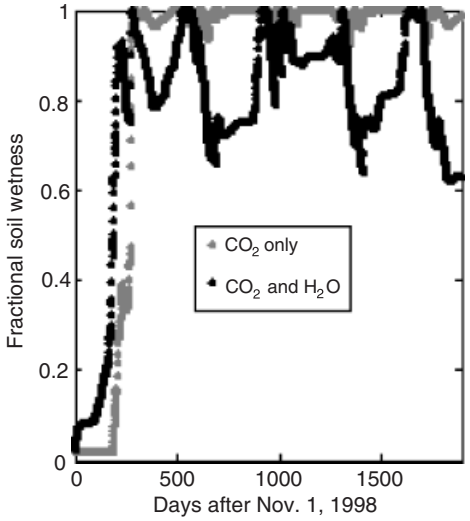

Fig. 4 Modeled soil water content of the root zone, expressed as a fraction of soil water-holding capacity. The base model was run using the optimized parameter set from either the optimization on CO_2 fluxes only, or the optimization on CO_2 and H_2O fluxes. The optimization on CO_2 only predicts almost no soil water drawdown, an unrealistic result. In the optimization on both fluxes, soil water is drawn down in the growing season from transpiration, and is replenished in the winter from snow melt. This greater drawdown has a significant effect on soil respiration, which is linearly related to fractional soil wetness in the model.

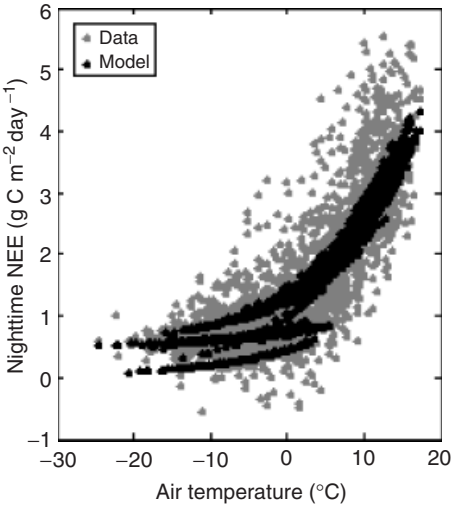

Fig. 5 Observed and modeled night-time respiration rates vs. air temperature, where model output is from the base model using the best parameter set retrieved from the optimization. Although soil respiration is dependent on soil temperature rather than air temperature, for clarity only air temperature is shown as an independent variable. Note that these data are presented as daily rates rather than as totals over each time step (as is done elsewhere). The two lower, nearly horizontal regions represent times when the soil is frozen, shutting down foliar respiration. The lower of these two regions represents an additional decrease in soil respiration because of dry soils (which, in the model, only occurs during the first few months of the simulation).

seasonal R_H model predicts more negative NEE (less respiration) during the growing season, and more positive NEE (more respiration) outside the growing season (Fig. 10).

The Lloyd-and-Taylor model did not, however, lead to a significantly different maximum likelihood from that of the base model (Table 3). Thus, simply using a function that causes a continuous increase in the temperature sensitivity of soil respiration with decreasing temperatures does not allow a better model-data fit. More substantial changes – such as allowing seasonally varying respiration parameters – are needed to achieve this better fit. This is consistent with observations at the site that both substrate type and microbial communities differ between the seasons, which might cause a discontinuous response rather than one continuously scaled to temperature (Lipson *et al*., 2002; Scott-Denton *et al*., 2005).

The optimization on the litter model actually yielded a worse model-data fit than that on the base model (Table 3). If the parameters are unbounded, adding extra free parameters can only lead to an improvement in fit. Specifying bounds on the parameters, however, can force a worse fit, and this is what happened in our experiment. The two parameters governing litter respiration rate (K_B and F_R) were both estimated at the lower ends of their range (yielding low litter respiration), implying that if their ranges were widened, the retrieved values would be even lower. In fact, even with the specification of lower bounds on these parameters, the total litter respiration in the optimized model ended up being a small fraction (about 5%) of the total heterotrophic respiration. This result suggests that a more complex model structure is required to capture the subtle effects of litter decomposition and soil carbon fractionation. Because of the even greater dimensionality this will introduce, additional data constraints will also likely be required, such as litter decomposition and isotopic data (Ryan & Law, 2005).

Finally, the optimization on the moisture-independent R_H model performed only slightly worse than that on the base model (Table 3). Possible reasons for this are discussed below in the section on including water vapor fluxes in the optimization.

Discussion

Parameter estimates

Some retrieved parameter values (Table 4) were significantly different from values measured in the field. This

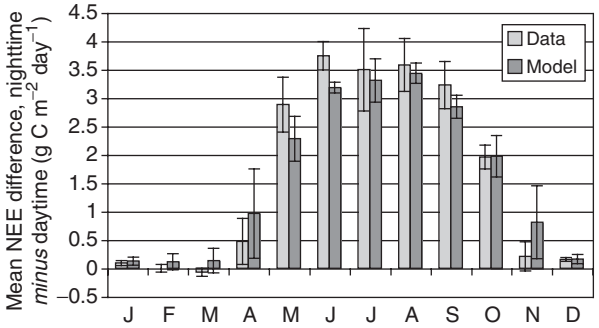

Fig. 6 Monthly mean diurnal cycle (night-time net ecosystem exchange of CO_2 (NEE) minus daytime NEE) in observations and optimized base model. Error bars show one standard deviation of the five (for January–October, 1999–2003) or six (for November and December, 1998–2003) annual means for each month. Positive NEE denotes net loss of CO_2 from the ecosystem to the atmosphere.

was often because of correlations between parameters (Fig. 8). For example, the retrieved value for $C_{L,0}$, the initial stock of leaf carbon (564 g C m^{-2}), is significantly less than the measured value of 1700 g C m^{-2} (unpublished data). If all other parameters were held constant, this difference would lead to a large under prediction of net photosynthesis. However, the retrieved value of $C_{L,0}$ was strongly correlated with A_{max} ($r = -0.96$). Thus, a higher value of A_{max} could compensate for the lower value of $C_{L,0}$. Indeed, our retrieved value for A_{max} (7.66 nmol CO_2 g^{-1} s^{-1}) is higher than the measured value for the site (4.5 nmol CO_2 g^{-1} s^{-1}; Huxman *et al.*, 2003). In addition, the retrieved value of $PAR_{1/2}$ (7.9 mol m^{-2} day^{-1}) gives higher rates of photosynthesis than the value reported by Aber *et al.* (1996) for needle-leaf evergreen forests (17 mol m^{-2} day^{-1}). These trade-offs illustrate that the optimized model can sometimes achieve the right answer (i.e. the right fluxes) for the wrong reason (i.e. using the wrong parameter values).

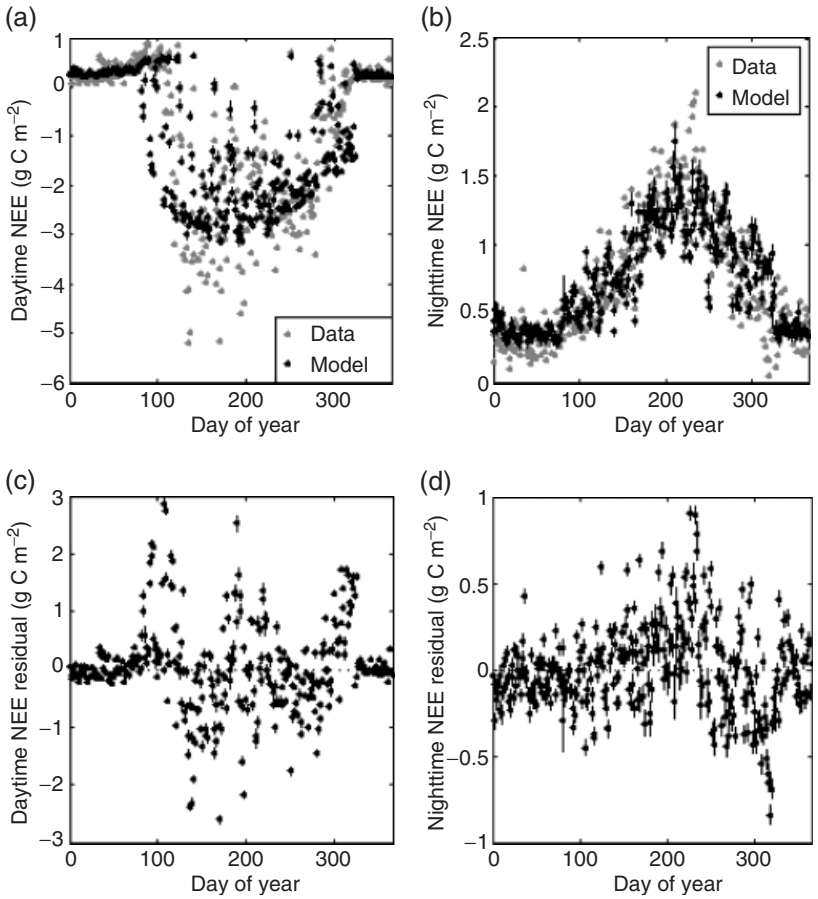

Fig. 7 Confidence intervals on one representative year (2001) of net ecosystem exchange of CO_2 (NEE) estimates from the optimization on the base model. Points show the mean and error bars show two standard deviations across the entire ensemble of parameter sets retrieved from the optimization ($n = 168\,150$). (a) and (b) show the modeled and observed NEE time series for daytime and night-time points, respectively. (c) and (d) show the daytime and night-time residuals (data minus model), respectively. Positive NEE denotes net loss of CO_2 from the ecosystem to the atmosphere.

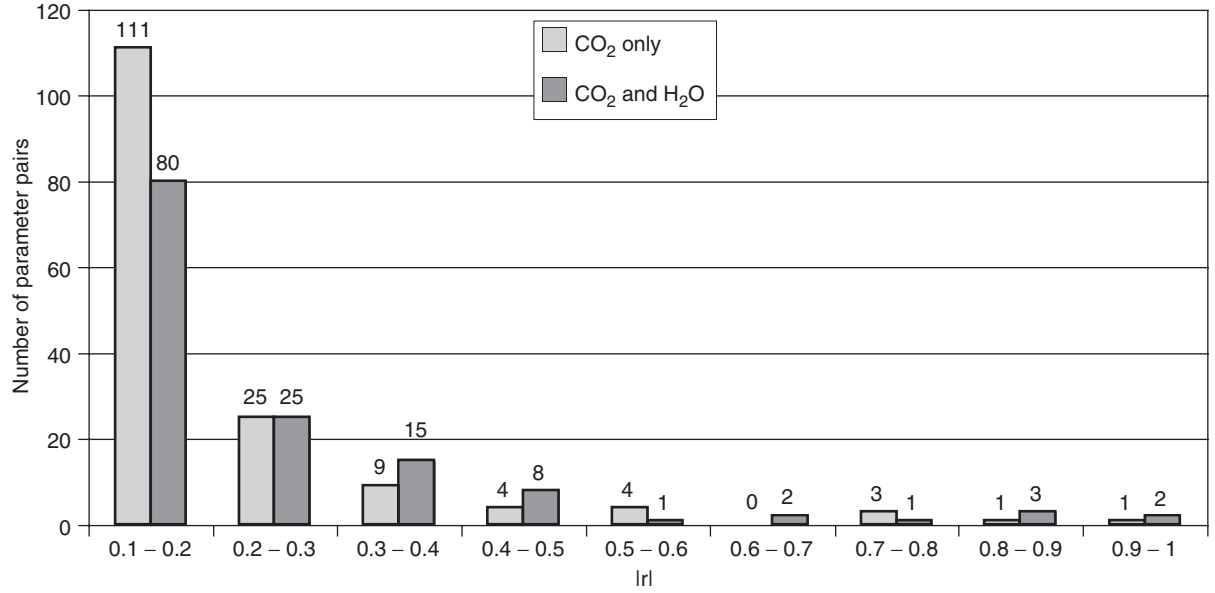

Fig. 8 Number of pair-wise parameter correlations with different levels of linear correlation coefficients, for the optimization on CO_2 fluxes only and the optimization on both CO_2 fluxes and H_2O fluxes. The number of parameter pairs with $|r| < 0.1$ was 338 for the optimization on CO_2 only and 359 for the optimization on CO_2 and H_2O. The most highly correlated parameters were, for the optimization on CO_2 only, $C_{L,0}$ and A_{max} ($r = -0.96$), $C_{S,0}$ and K_H ($r = -0.89$), NPP_L and K_L ($r = 0.75$), $PAR_{1/2}$ and SLW_C ($r = 0.74$), and $C_{W,0}$ and K_A ($r = -0.73$), and, for the optimization on CO_2 and H_2O, K_S and R_d ($r = 1.0$; however, this was because of little or no variation in the retrieved values of these two parameters), $C_{L,0}$ and A_{max} ($r = -0.91$), f and $W_{R,c}$ ($r = -0.89$), $C_{W,0}$ and K_A ($r = -0.87$), $PAR_{1/2}$ and SLW_C ($r = 0.86$), and NPP_L and K_L ($r = 0.79$).

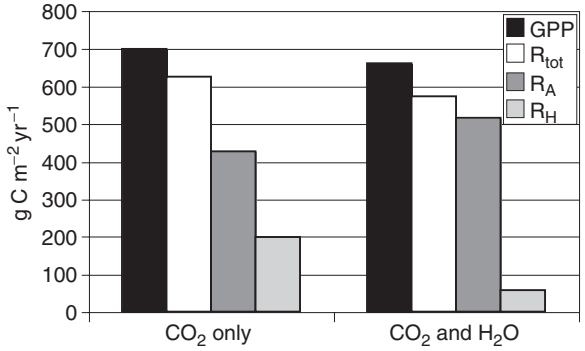

Fig. 9 Mean annual breakdown of net ecosystem exchange of CO_2 into component fluxes, as predicted by the base model run using the best parameter set retrieved from the optimization on CO_2 fluxes only and from the optimization on both CO_2 fluxes and H_2O fluxes. GPP is the gross primary productivity, R_{tot} is the total ecosystem respiration, R_A is the autotrophic respiration, and R_H is the heterotrophic respiration.

Using a synthetic data set generated with known parameter values, however, Braswell *et al*. (2005) found that this optimization approach applied to a similar model was able to retrieve nearly correct values for the majority of the parameters. This conclusion held even when a relatively large white noise was added to the data. Thus, with the exception of parameters that are highly correlated, the parameter optimization seems able to retrieve the correct (i.e. truly optimal) values of most parameters. However, the optimal values at the spatial scale of the tower footprint and the temporal scale of half a day may differ from values measured in the lab, or values measured at a smaller scale in the field.

Diagnosing systematic errors

The optimized model is able to capture the basic cyclic controls on NEE (diurnal and seasonal) in this ecosystem, but it still fails to capture many of the sources of variability. This is especially apparent for night-time respiration (Fig. 5). Although the model does a good job of predicting the observed temperature sensitivity of respiration, there is much more variation in observed than in predicted NEE. The variation in observed NEE is present even within a given year, so interannual variability alone cannot explain the model-data mismatch. One likely cause of this variability is changes in substrate availability (Giardina & Ryan, 2000; Ryan & Law, 2005). Scott-Denton *et al*. (2005) have shown that the types of substrates available to drive both the heterotrophic and rhizospheric components of soil re-

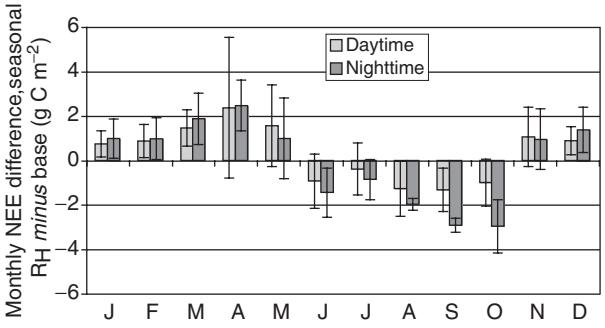

Fig. 10 Differences in the mean monthly net ecosystem exchange of CO_2 (NEE) predictions between the optimized base model and the optimized seasonal R_H model (expressed as seasonal R_H minus base). Error bars show one standard deviation of the five (for January–October, 1999–2003) or six (for November and December, 1998–2003) annual means for each month. Positive NEE denotes net loss of CO_2 from the ecosystem to the atmosphere.

spiration vary seasonally and interannually, and vary with regard to their effects on either component. We attempted to better model these changes in substrate availability, and the resulting additional dynamics of soil respiration, by splitting the soil into a fast-turnover litter pool and a slow-turnover soil pool. The simple modification applied here, however, did not allow an improvement in model-data fit (Table 3). The fact that the optimization forced the respiration of the new litter pool to near-zero also indicates that the manner in which we represented turnover of the different pools was too simple and thus unrealistic. One of the surprising results to emerge from the study by Scott-Denton *et al*. (2005) is the presence of relatively high concentrations of tree-derived sucrose in the soil during the winter. The presence of such a labile carbon source at a time when the photosynthetic activity of the forest is at a minimum is not captured in the current model. It is likely that the sucrose is used in winter freeze protection and leaks from the shallow roots as a result of wintertime mechanical damage. A more realistic soil pool parameterization will require more explicit representation of rhizospheric control over specific dissolved organic compounds in the soil.

One of the most noticeable errors in the optimized model predictions is that they underestimate mid-summer night-time respiration (Figs 2b and 3d). This error could arise because two different temperature sensitivities – intraseasonal and interseasonal – are modeled using a single Q_{10} value in the base model. Specifically, the fact that the model underestimates respiration when the soil temperatures are warmest suggests that the optimized intraseasonal temperature sensitivity is too low. This could occur if the optimum interseasonal temperature sensitivity is lower than the optimum intraseasonal sensitivity, forcing the single Q_{10} to compromise between the two. One possible cause for differences between seasons is that there may be different soil microbial communities in the summer and winter, as suggested by Lipson *et al*. (2002). Another possibility, as mentioned above, is missing substrate dynamics in the model, such as the presence of high concentrations of tree-derived sucrose in the winter (Scott-Denton *et al*., 2005). The fact that the seasonal R_H model was able to match the data better than the base model lends support to at least one of these hypotheses.

The parameter values retrieved from the optimization on the seasonal R_H model suggest that there is, indeed, higher temperature sensitivity within seasons than between seasons. The optimum values of both Q_{10} values (for warm soil and cold soil) are higher than the optimum value for the single Q_{10} in the base model. Furthermore, the base respiration rate (at 0 °C) in cold soils is about three times higher than the base rate in warm soils (Table 5). This could indicate that there is more substrate available in the winter, and that this effect is not captured by the model's dynamics. Recent observations by Scott-Denton *et al*. (2005) have shown that soil microbial biomass exhibits both winter and summer maxima and, as discussed above, soil-dissolved organic carbon concentrations generally, and sucrose concentrations specifically, are relatively high during the winter. These observations are not represented in the current version of the model.

Table 5 Heterotrophic respiration parameters retrieved from optimization on model with seasonally varying R_H

Parameter	Best value	Mean value
$K_{H,w}$ (g C g^{-1} C yr^{-1})	0.006	0.007 ± 0.001
$K_{H,c}$ (g C g^{-1} C yr^{-1})	0.017	0.020 ± 0.005
$Q_{10S,w}$	1.91	2.08 ± 0.36
$Q_{10S,c}$	5.75	5.07 ± 0.75
T_c(°C)	0.42	0.41 ± 0.01

$K_{H,w}$ and $K_{H,c}$ are the base respiration rates at 0 °C and with moisture-saturated soil for warm and cold soils, respectively. $Q_{10S,w}$ and $Q_{10S,c}$ are the respiration Q_{10S} for warm and cold soils, respectively. T_c is the temperature below which the cold soil parameters are used. The 'Best value' column reports the parameter values from the parameter set that yielded the highest likelihood in the Markov chain Monte Carlo parameter estimation. The 'Mean value' column reports the estimated posterior mean and standard deviation of each parameter, generated from 152 382 parameter sets that yielded approximately equally good model-data fits. For comparison, the parameter optimization on the base model yielded optimum values of K_H and Q_{10}s of 0.009 g C g^{-1} C yr^{-1} and 1.50, respectively.

It is interesting to note, however, that the changes in the mean monthly night-time NEE with seasonally varying soil respiration (Fig. 10) are often in the opposite direction of what would be needed to correct for the mean monthly error between the base model and the data (Fig. 2b). In contrast, these changes in the mean monthly NEE are usually in the right direction to correct (partially) the daytime errors. This could indicate that at least some of the improvement observed with the seasonal R_H model may be correcting for model errors in other flux components, such as photosynthesis.

Effects of including water vapor fluxes in optimization

Including H_2O fluxes in the optimization did not provide additional information about the separation of NEE into GPP and R (Fig. 9). This suggests that this partitioning is already near-optimal because SIPNET models daytime and night-time fluxes separately. As parameters governing GPP have no direct influence over night-time NEE, night-time data provide a strong constraint only on parameters governing R. Daytime data provide a strong constraint on GPP-related parameters, and probably provide a relatively weaker constraint on R-related parameters. Thus, it is instructive to think of the optimization as occurring in two steps: night-time fluxes determine the R-related parameters and then, given these R-related parameters as fixed, daytime fluxes determine the GPP-related parameters. (However, it is important to note that, in reality, both daytime and night-time data are considered simultaneously in the optimization, assuring consistency between the optimized GPP and R-related parameters.) Thus, by modeling daytime and night-time fluxes separately and considering both sets of fluxes in the optimization, we are able to separate NEE into GPP and R, even when only CO_2 fluxes are used in the optimization.

Similarly, including H_2O fluxes in the optimization did not lead to lower pair-wise parameter correlations (Fig. 8). In the optimization on the base model, there were no instances of high correlations between a GPP-related parameter and an R-related parameter; one would expect to see such correlations if the model was run at a time step of days or longer. In the case of correlations between two R-related parameters, neither parameter will have any direct effect on evapotranspiration, so H_2O fluxes can provide little information to break these correlations. GPP-related parameters, on the other hand, have the same effect on transpiration as on photosynthesis (in the absence of water stress), so again, H_2O fluxes can provide little information to break correlations between two GPP-related parameters. Thus, the addition of H_2O fluxes in the optimization provides information mainly about parameters that directly govern evapotranspiration in the model.

Including H_2O fluxes in the optimization did, however, lead to differences in the optimal separation of R into R_A and R_H, with more R_A and less R_H (Fig. 9). As these data can provide no direct information about R, the decrease in R_H is because of indirect effects. These effects are imposed through differences in the optimized soil moisture dynamics when H_2O fluxes are included in the optimization. In the optimization on CO_2 alone, soil moisture remains fairly constant over time; in the optimization on both fluxes, soil moisture is more variable (Fig. 4). The soil moisture dynamics imposed by optimizing on H_2O fluxes are different from those needed to describe correctly the effects of soil moisture stress on soil respiration. Thus, in order to match both the observed H_2O fluxes and the observed CO_2 fluxes, R_H must be decreased to reduce the impact of this erroneous representation. However, measured soil wetness for 2002 and 2003 at the site shows patterns more similar to the optimization on both fluxes (data not shown). Thus, the decrease in R_H when soil moisture is more variable indicates *not* that this increased variability is incorrect, but that it is incorrect to model R_H using a linear dependence on fractional soil wetness at this site Eqn (A2).

For similar reasons, the optimum model-data fit did not change significantly when R_H was made independent of soil moisture (Table 3). Although we expected this modification to lead to a greater model-data mismatch, this result is not too surprising given that the optimized base model showed little or no water stress on heterotrophic respiration throughout most of the simulation (Fig. 4). Again, this does not imply that soil moisture has no effect on heterotrophic respiration at this site. Rather, the linear dependence used in SIPNET Eqn (A2) seems to be the wrong model for this dependence. Lee *et al*. (2004) have shown, for example, that soil respiration responds relatively quickly and transiently to precipitation events. At the Niwot Ridge site, observations have shown that although soil respiration is dependent on soil moisture, this is primarily an interannual dependence, not a seasonal dependence, despite the large seasonal variability in soil moisture (Monson *et al*., 2002; Scott-Denton *et al*., 2003; Scott-Denton *et al*., 2005). More complex processes and interactions may control interannual variation (Schimel *et al*., 2005; Ryan & Law, 2005). It is possible, for instance, that the observed effects of soil moisture on soil respiration are due more to indirect effects on substrate availability than direct effects of climate. For example, wetter soils may allow greater photosynthesis, which stimulates soil respiration by providing more carbon directly to the

rhizospheric community and indirectly to the heterotrophic component (in the form of root turnover).

Conclusions

This modeling study at Niwot Ridge demonstrates that model-data synthesis can increase the usefulness of eddy covariance flux measurements for understanding respiration. Optimization of model parameters in a process model is a strong alternative approach to statistical curve fitting for partitioning NEE into its component fluxes. In doing so, the partitioning is clearly traceable to specific biological assumptions and can incorporate dynamic responses of the system. There are strong reasons for beginning the model-fitting procedure with a simplified model, allowing model-data mismatches to guide model development. This iterative approach allows a fairly direct assessment of which processes the data do and do not constrain. When performing a parameter estimation, the model's dimensionality should be carefully assessed relative to the dimensionality in the data to avoid overfitting. It is probably counterproductive to begin with a model so complex that the initial fit lacks systematic error; instead, it is critical to maintain a model structure that is falsifiable and this is difficult if the initial model is subject to overfitting.

By coupling a parameter optimization with a formal model selection criterion, we were able to test hypotheses by making small modifications to the base model and examining their effects on the optimized model-data fit. One key finding that emerged from such an experiment is that photosynthesis, and possibly foliar respiration, are shut down when the soil is frozen in this evergreen forest. This result supports similar findings reported by Hollinger *et al*. (1999) and Monson *et al*. (2002). Another result that emerged from a model modification experiment is that the metabolic responses of the microbial community in the summer and winter probably vary, supporting findings by Lipson *et al*. (2002) and D. A. Lipson *et al*. (unpublished data). Summer respiration may be largely driven by exudation of labile compounds into the soil by roots, while wintertime respiration may derive more from longer-lived compounds. However, at least some of the improvement observed with this model modification may have been correcting for errors in other model components, such as photosynthesis. Furthermore, although including a seasonal effect on R_H parameters reduced model error, substantial unexplained variability in respiration remained. Recent literature indicating a tight coupling between plant timing of root exudation and respiration suggests that a new type of allocation model may be needed to improve this aspect of the model fit (Ryan & Law, 2005).

The application of optimization and data assimilation techniques has emphasized the use of CO_2 concentration and flux data but several papers emphasize the simultaneous use of multivariate data: the so-called 'multiple constraints' approach (Barrett, 2002; Reichstein *et al*., 2003; Wang & Barrett, 2003). While in the long run the use of multiple constraints is essential, in this study a straightforward addition of a second key data set (H_2O flux) did not aid in the accurate modeling of CO_2 fluxes, and by some measures actually degraded the solution. This likely reflects – in part – the lack of independence in the data and data errors (as both flux measurements are made using the eddy covariance technique). Next-generation multiple constraint models will require a much more sophisticated treatment of data error and error covariance.

The next challenge in model-data synthesis is to diagnose explicitly controls over long-term variability. Work to date (Braswell *et al*., 2005; this work) has provided an improved quantitative understanding of controls on the diurnal and seasonal time scales and clarifies several issues critical for moving to longer time scales, such as controls over plant and soil respiration linked to seasonality. However, direct analysis of interannual and longer-term variability will require adding key mechanisms, longer data records, and a multiple constraints approach. It is likely that an interannual model will have to include a process-level allocation scheme (Ryan & Law, 2005) and a nitrogen cycle (Schimel *et al*., 2005). Additional data constraints for longer time scales may include dendrochronology, allocation and litterfall data, isotopic allocation and turnover estimates, and soil carbon fraction and biomass increment measurements. It can be difficult to separate the effects of substrate dynamics from those of environmental controls on respiration and photosynthesis, because these fluxes depend on the product of these two types of effects. The incorporation of measurements of substrate dynamics into a model-data synthesis will allow this separation. However, while multiple constraints will be needed to simulate and diagnose interannual and decadal variability, we caution that care must be exercised in fitting and diagnosis, especially when additional data sets are not statistically independent of each other.

Acknowledgments

We are grateful for Ernst Linder's help with the statistics underlying the parameter estimation. We also thank Sean Burns, Andrew Turnipseed, and others who were instrumental in the data collection. Finally, we thank Beverly Law and four anon-

ymous reviewers for comments that led to a greatly improved manuscript. This work was supported by grants from the National Aeronautics and Space Administration (TE/02-0000-0015), the National Science Foundation (2003108), and the National Oceanic and Atmospheric Administration (2002192). The National Center for Atmospheric Research is funded by the National Science Foundation.

References

Aber JD, Federer CA (1992) A generalized, lumped-parameter model of photosynthesis, evapo-transpiration and net primary production in temperate and boreal forest ecosystems. *Oecologia*, **92**, 463–474.

Aber JD, Ollinger SV, Driscoll CT (1997) Modeling nitrogen saturation in forest ecosystems in response to land use and atmospheric deposition. *Ecological Modelling*, **101**, 61–78.

Aber JD, Ollinger SV, Federer CA *et al*. (1995) Predicting the effects of climate change on water yield and forest production in the northeastern United States. *Climate Research*, **5**, 207–222.

Aber JD, Reich PB, Goulden ML (1996) Extrapolating leaf CO_2 exchange to the canopy: a generalized model of forest photosynthesis validated by eddy correlation. *Oecologia*, **106**, 257–265.

Baldocchi DD (2003) Assessing the eddy covariance technique for evaluating carbon dioxide exchange rates of ecosystems: past present and future. *Global Change Biology*, **9**, 479–492.

Baldocchi DD, Falge E, Gu L *et al*. (2001) FluxNet: a new tool to study the temporal and spatial variability of ecosystem-scale carbon dioxide, water vapor and energy flux densities. *Bulletin of the American Meteorological Society*, **82**, 2415–2434.

Baldocchi DD, Hicks BB, Meyers TP (1988) Measuring biosphere-atmosphere exchanges of biologically related gases with micrometeorological methods. *Ecology*, **69**, 1331–1340.

Baldocchi DD, Wilson KB (2001) Modeling CO_2 and water vapor exchange of a temperate broadleaved forest across hourly to decadal time scales. *Ecological Modelling*, **142**, 155–184.

Barrett DJ (2002) Steady state turnover time of carbon in the Australian terrestrial biosphere. *Global Biogeochemical Cycles*, **16**, 1108, doi: 10.1029/2002GB001860.

Bishop C (1995) *Neural Networks for Pattern Recognition*. Oxford University Press, New York.

Braswell BH, Sacks WJ, Linder E *et al*. (2005) Estimating diurnal to annual ecosystem parameters by synthesis of a carbon flux model with eddy covariance net ecosystem exchange observations. *Global Change Biology*, **11**, 335–355.

Falge E, Baldocchi D, Olson R *et al*. (2001) Gap filling strategies for defensible annual sums of net ecosystem exchange. *Agricultural and Forest Meteorology*, **107**, 43–69.

Gershenfeld N (1999) *The Nature of Mathematical Modeling*. Cambridge University Press, Cambridge.

Giardina CP, Ryan MG (2000) Evidence that decomposition rates of organic carbon in mineral soil do not vary with temperature. *Nature*, **404**, 858–861.

Goulden ML, Munger JW, Fan SM *et al*. (1996) Measurements of carbon sequestration by long-term eddy covariance: methods and a critical evaluation of accuracy. *Global Change Biology*, **2**, 169–182.

Hanson PJ, Edwards NT, Garten CT *et al*. (2000) Separating root and soil microbial contributions to soil respiration: a review of methods and observations. *Biogeochemistry*, **48**, 115–146.

Högberg P, Nordgren A, Buchmann N *et al*. (2001) Large-scale forest girdling shows that current photosynthesis drives soil respiration. *Nature*, **411**, 789–792.

Hollinger DY, Goltz SM, Davidson EA *et al*. (1999) Seasonal patterns and environmental control of carbon dioxide and water vapour exchange in an ecotonal boreal forest. *Global Change Biology*, **5**, 891–902.

Hurtt GC, Armstrong RA (1996) A pelagic ecosystem model calibrated with BATS data. *Deep-Sea Research Part II-Topical Studies in Oceanography*, **43**, 653–683.

Huxman TE, Turnipseed AA, Sparks JP *et al*. (2003) Temperature as a control over ecosystem CO_2 fluxes in a high-elevation, subalpine forest. *Oecologia*, **134**, 537–546.

Kendall MG, Ord JK (1990) *Time Series*. Oxford University Press, New York.

Lee X, Wu H-J, Sigler J *et al*. (2004) Rapid and transient response of soil respiration to rain. *Global Change Biology*, **10**, 1017–1026.

Lipson DA, Schadt CW, Schmidt SK (2002) Changes in microbial community structure and function following snow melt in an alpine soil. *Microbial Ecology*, **43**, 307–314.

Lloyd J, Taylor JA (1994) On the temperature dependence of soil respiration. *Functional Ecology*, **8**, 315–323.

MacKay DJC (1992) A practical Bayesian framework for back-propagation networks. *Neural Computation*, **4**, 448–472.

Metropolis N, Rosenbluth AW, Rosenbluth MN *et al*. (1953) Equations of state calculations by fast computing machines. *Journal of Chemical Physics*, **21**, 1087–1092.

Mikan CJ, Schimel JP, Doyle AP (2002) Temperature controls of microbial respiration above and below freezing in arctic tundra soils. *Soil Biology & Biogeochemistry*, **34**, 1785–1795.

Monson RK, Turnipseed AA, Sparks JP *et al*. (2002) Carbon sequestration in a high-elevation, subalpine forest. *Global Change Biology*, **8**, 459–478.

Raich JW, Rastetter EB, Melillo JM *et al*. (1991) Potential net primary productivity in South-America: application of a global model. *Ecological Applications*, **1**, 399–429.

Raupach MR, Rayner PJ, Barrett DJ *et al*. (2005) Model-data synthesis in terrestrial carbon observation: methods, data requirements and data uncertainty specifications. *Global Change Biology*, **11**, 378–397.

Reichstein M, Tenhunen J, Roupsard O *et al*. (2003) Inverse modeling of seasonal drought effects on canopy CO_2/H_2O exchange in three Mediterranean ecosystems. *Journal of Geophysical Research*, **108**, 4726, doi: 10.1029/2003JD003430.

Ryan MG, Law BE (2005) Interpreting, measuring and modeling soil respiration. *Biogeochemistry*, **73**, 3–27.

Schimel DS, Churkina G, Braswell BH (2005) Remembrance of weather past: time scales, time lags, complex dynamics and net ecosystem exchange. In: *A History of Atmospheric CO_2 and its Effects on Plants, Animals, and Ecosystems* (eds Ehleringer J, Cerling T, Dearing D), Springer-Verlag, New York.

Schulz K, Jarvis A, Beven K (2001) The predictive uncertainty of land surface fluxes in response to increasing ambient carbon dioxide. *Journal of Climate*, **14**, 2551–2562.

Scott-Denton LE, Rosenstiel TN, Monson RK (2005) Differential controls over the heterotrophic and rhizospheric components of soil respiration in a high-elevation, subalpine forest. *Global Change Biology*, doi:10.1111/j.1365–2486.2005.01064.x

Scott-Denton LE, Sparks KL, Monson RK (2003) Spatial and temporal controls of soil respiration rate in a high-elevation, subalpine forest. *Soil Biology & Biogeochemistry*, **35**, 525–534.

Sellers PJ, Heiser MD, Hall FG (1992) Relationship between surface conductance and spectral vegetation indices at intermediate ($100\,m^2$–$15\,m^2$) length scales. *Journal of Geophysical Research, FIFE Special Issue*, **97**, 19033–19060.

Sellers PJ, Randall DA, Collatz GJ *et al*. (1996) A revised land surface parameterization (SiB_2) for atmospheric GCMs. Part I: model formulation. *Journal of Climate*, **9**, 676–705.

Subke J-A, Hahn V, Battipaglia G *et al*. (2004) Feedback interactions between needle litter decomposition and rhizospheric activity. *Oecologia*, **139**, 551–559.

Turnipseed AA, Anderson DE, Blanken PD *et al*. (2003) Airflows and turbulent flux measurements in mountainous terrain. Part 1: canopy and local effects. *Agricultural and Forest Meteorology*, **119**, 1–21.

Turnipseed AA, Anderson DE, Burns S *et al*. (2004) Airflows and turbulent flux measurements in mountainous terrain. Part 2: mesoscale effects. *Agricultural and Forest Meteorology*, **125**, 187–205.

Turnipseed AA, Blanken PD, Anderson DE *et al*. (2002) Energy budget above a high-elevation subalpine forest in complex topography. *Agricultural and Forest Meteorology*, **110**, 177–201.

van Wijk MT, Bouten W (2002) Simulating daily and half-hourly fluxes of forest carbon dioxide and water vapor exchange with a simple model of light and water use. *Ecosystems*, **5**, 597–610.

Wang YP, Barrett DJ (2003) Estimating regional terrestrial carbon fluxes for the Australian continent using a multiple-constraint approach I. Using remotely sensed data and ecological observations of net primary production. *Tellus (B)*, **55**, 270–289.

Wang YP, Leuning R, Cleugh HA *et al*. (2001) Parameter estimation in surface exchange models using nonlinear inversion: how many parameters can we estimate and which measurements are most useful? *Global Change Biology*, **7**, 495–510.

Appendix: Model Description

SIPNET contains two vegetation carbon pools (leaves and wood) and an aggregated soil carbon pool, as well as a soil moisture submodel (Fig. 1). We ran the model at a twice-daily time step, with one time step for each day or night. The initial conditions and fluxes are governed by 35 parameters (Tables 1 and 2). An earlier version of SIPNET, which was applied to a deciduous forest in the northeastern US, is described by Braswell *et al*. (2005). Here, we summarize the major components of the model and describe in detail the changes that have been made in applying it to the Niwot Ridge evergreen forest.

Gross photosynthesis (GPP) in SIPNET is determined as in PnET (Aber & Federer, 1992), as an unstressed rate modified by four factors, each between 0 and 1: an air temperature factor, a VPD factor, a light factor, and a water stress factor. Photosynthesis is assumed to respond quadratically to air temperature, reaching an optimum at T_{opt} and falling to zero below T_{min}. Photosynthesis also decreases with VPD^2, where VPD is the atmospheric vapor pressure deficit; the slope of this relationship is determined by K_{VPD}. The light factor expresses the amount of light falling on the leaves as a fraction of the saturated light level. This factor is determined both by the amount of light falling on the top of the canopy (PAR) and by the attenuation of light through the canopy. Light attenuation is computed as an exponential decay function, assuming that the vertical distribution of leaf area is homogenous through the canopy. After these three stress factors are applied, a transpiration demand is computed based on the modified GPP, the atmospheric VPD, and K_{WUE}. If the amount of plant-available soil water, calculated as $W_R f$ (where W_R is the amount of water in the root zone and f is a constant), is less than the transpiration demand, then both photosynthesis and transpiration are further decreased by the ratio of available water to transpiration demand.

Unlike the original version of SIPNET, which used a deciduous phenology (Braswell *et al*., 2005), the version of the model used in this study uses an evergreen leaf phenology. At each time step, leaf carbon is added by an amount proportional to the mean NPP over the last 5 days. Carbon is lost from the leaves and transferred to the soil using a constant turnover rate. As in the previous version of SIPNET, wood carbon is also transferred to the soil using a constant turnover rate.

Autotrophic respiration in SIPNET is the sum of two terms: wood maintenance respiration and foliar respiration. Growth respiration is implicitly included in these terms, both to keep the initial model as simple as possible and because we did not feel that there was enough information in the flux data to separate out these three types of respiration. Both wood and foliar respiration are modeled as

$$R_x = K_x C_x f(T_{air}), \tag{A1}$$

where R_x is the realized respiration rate, K_x is a base rate, C_x is the carbon in the given pool (either wood or leaves), T_{air} is the air temperature, and f is an exponential function. Both respiration fluxes use the same Q_{10} value to relate respiration to temperature (Q_{10V}). Note that the wood pool in the model represents all wood, which has the somewhat unrealistic corollary that dead wood respires. However, this should not lead to large errors as long as the base respiration rate is expressed as g C respired per g biomass (rather than per g live wood), and as long as the ratio of live wood to total

wood does not change significantly over the course of the simulation. This method of modeling wood maintenance respiration has been used in other ecosystem models, such as TEM (Raich *et al*., 1991).

Soil respiration, which represents the respiration of heterotrophic microbes in the model's single aggregated soil pool, is modeled in a manner similar to autotrophic respiration. A base rate is multiplied by the amount of carbon in the substrate, and then modified by an exponential function of soil temperature. The Q_{10} value used for this function is different from that used for autotrophic respiration. Soil respiration is also modified by a soil wetness function, increasing linearly with soil moisture (Aber *et al*., 1997), yielding:

$$R_H = K_H C_S f(T_{soil})(W_R/W_{R,C}), \quad \text{(A2)}$$

where R_H is the realized soil respiration rate, K_H is the base rate, C_S is the amount of carbon in the soil pool, T_{soil} is the soil temperature, W_R is the amount of water in the root zone, and $W_{R,c}$ is the water-holding capacity of the root zone. Note that we assume that soil respiration is independent of the surface layer wetness.

The most significant change made in this version of the model was the inclusion of a more complex water routine (Fig. 1). At Niwot Ridge, soil moisture is thought to be a significant determinant of NEE (Monson *et al*., 2002); at Harvard Forest, in contrast, vegetation is thought to experience relatively less water stress (Aber *et al*., 1995). In addition, snowmelt dynamics have a significant effect on NEE at Niwot Ridge (Monson *et al*., 2002); consequently, we added a snow accumulation and melt model to SIPNET.

If the air temperature is above 0 °C precipitation falls as rain, with some fraction (E) immediately intercepted and evaporated before entering the soil (the immediate evaporation flux, E_I). An additional fraction (F) of rain and snow melt (described below) goes directly to drainage (Aber *et al*., 1995). The remainder is assumed to infiltrate the soil water surface layer.

If the air temperature is below 0 °C precipitation falls as snow and accumulates in a snow pack. Sublimation from the snow pack is based on the equation used in the SiB2 model (Sellers *et al*., 1996, their Eqn (33b)):

$$E_P = \frac{e^*(0\,^\circ\mathrm{C}) e_a}{r_d} \frac{\rho c_p}{\gamma} \frac{1}{\lambda_s}, \quad \text{(A3)}$$

where E_P is sublimation from the snow pack, e^* (0 °C) is the saturation vapor pressure at 0 °C (the assumed temperature of the snow pack), e_a is the atmospheric vapor pressure, ρ is the density of air, c_p is the specific heat of air, γ is the psychrometric constant, λ_s is the latent heat of sublimation, and r_d is the aerodynamic resistance between the ground and the canopy air space, which decreases with wind speed:

$$r_d = \frac{R_d}{u}, \quad \text{(A4)}$$

where R_d is assumed to be constant and is estimated in the parameter optimization, and u is the wind speed. When the air temperature is above 0 °C, snow melts at a rate proportional to air temperature.

Evaporation from the soil water surface layer is also based on the equation used in the SiB2 model (Sellers *et al*., 1996, their Eqn (34)):

$$E_S = \frac{e^*(T_{soil}) - e_a}{r_{soil} + r_d} \frac{\rho c_p}{\gamma} \frac{1}{\lambda}, \quad \text{(A5)}$$

where E_S is soil evaporation, e^* (T_{soil}) is the saturation vapor pressure at the temperature of the soil, λ is the latent heat of vaporization, r_{soil} is a soil resistance term, and all other symbols are as above. If there is a snow pack, soil evaporation is assumed to be zero. Sellers *et al*. (1996) multiply e^* (T_{soil}) by h_{soil}, the relative humidity of the soil pore space. We dropped this term to reduce the number of parameters in the model; h_{soil} is only significantly less than 1 when the soil is very dry, and in this case evaporation will be insignificant anyway. We compute r_{soil} using the functional form given by Sellers *et al*. (1992, their Eqn (19)):

$$r_{soil} = e^{R_{soil,1} - R_{soil,2} \cdot (W_s/W_{S,c})}, \quad \text{(A6)}$$

where $R_{soil,1}$ and $R_{soil,2}$ are constants estimated in the parameter optimization, W_S is the amount of water in the surface layer, and $W_{S,c}$ is the water-holding capacity of the surface layer, also estimated in the parameter optimization. Water drains from the surface layer to the root zone at a rate proportional to the surface layer wetness. Additional drainage occurs as necessary to keep the surface layer water content below its water-holding capacity.

Finally, transpiration removes water from the soil water root zone as in Braswell *et al*. (2005). Transpiration is the smaller of plant-available soil water and transpiration demand (see above). At the end of a time step, any water remaining in the root zone beyond its water-holding capacity is removed through drainage.